ELSEVIER

Chemical Engineering Journal 143 (2008) 1–9

Chemical Engineering Journal

www.elsevier.com/locate/cej

Review

Degradation of salicylic acid by Fenton and modified Fenton treatment

A. Goi [*], Y. Veressinina, M. Trapido

Department of Chemical Engineering, Tallinn University of Technology,
Ehitajate tee 5, Tallinn 19086, Estonia

Received 3 July 2007; received in revised form 11 September 2007; accepted 13 January 2008

Abstract

The degradation of salicylic acid (SA) was carried out utilizing classical Fenton reagents and modified Fenton with ferric iron salt and goethite as source of iron catalyst. The efficiency of the treatments was evaluated on the basis of SA degradation degree, COD and BOD reduction. Due to the tendency of SA to form complexes with ferric iron, decreasing the concentration of catalyst and increasing that of hydrogen peroxide intensified SA degradation by the classical Fenton process. Application of Fe^{3+}/H_2O_2 led to the same SA degradation degree as classical Fenton process with the following termination, where the entire residual SA is complexed with Fe^{3+}. SA degradation by modified Fenton was intensified with higher goethite concentration and in acidic pH conditions. The addition of UV-irradiation did not improve the action of the Fenton's/modified Fenton's reagent system. Overall COD and BOD removal efficiency comprised nearly 90% under optimal treatment conditions applied.

© 2008 Elsevier B.V. All rights reserved.

Keywords: Iron catalyst addition; Complex formation; Degradation degree; COD reduction

1. Introduction

Salicylic acid (SA), also known as 2-hydroxybenzoic acid (Fig. 1, I), is a colourless acicular crystal or a white crystalline powder [1]. SA in the form of esters was found in several plants, notably in wintergreen leaves and the bark of sweet birch [1]. It is produced synthetically by heating sodium phenolyate with carbon dioxide under pressure and microbial oxidation of naphthalene [2]. SA is a key additive in many skin-care ointments, creams, gels and transdermal patches [1]. Initially a concentration of 2% is used increasing to about 6% if necessary. SA is also a common chemical in dyes. Its derivatives of mordant azo dyes are numerically predominant and used mainly for orange and yellow hues [3]. It is often used in conjunction with many other agents, such as benzoic acid, coal tar, resorcinol and sulphur [1]. SA is also used in the form of collodion basis (10–17%) or as a plaster (20–50%) to destroy warts and corns [1]. The toxic effects of SA and salicylates are complex. Main risks with oral therapeutic doses are mostly gastrointestinal irritation. Due to the severe gastric irritation with SA causes, it is no longer used orally [1]. However, when used topically it may cause an allergic contact rash in some people. If applied to large areas of skin, it may be absorbed into the blood stream and induce salicylism [1].

Wastewater containing SA originates mainly from the synthesis of SA and its derivatives and from rinsing of medical and cosmetic manufacture equipment. This large variety of SA-contamination sources requires innovative water purification technologies. Advanced oxidation processes (AOP) that involve *in situ* generation of highly potent chemical oxidants such as the hydroxyl radicals have emerged as an important class of technologies for accelerating the oxidation and destruction of a wide range of organic contaminants in water and air [4]. The use of AOP in SA-contaminated water treatment is to date limited mainly to photocatalysis with TiO_2/UV or modified TiO_2/UV systems [5–9]. Concerning treatment processes using ozone, the application of some heterogeneous metal-supported catalysts were found to accelerate the ozonation efficacy of SA but resulted in considerably high ozone consumption [10,11]. Some other AOP, such as H_2O_2/UV/oxygen [12] and catalytic wet air oxidation with $LaFeO_3$ catalyst [13] have also shown different positive effects on SA-contaminated water purification.

Among AOP the application of Fenton's reagent for the destruction of water contaminants is one of the promising technologies because of the powerful oxidising potential and comparatively low cost. Iron (II) salts have traditionally been used as sources of iron catalyst because they provide near-stoichiometric generation of hydroxyl radicals from dilute H_2O_2

---

[*] Corresponding author. Tel.: +372 6204341; fax: +372 6202856.
E-mail address: goi@staff.ttu.ee (A. Goi).

1385-8947/$ – see front matter © 2008 Elsevier B.V. All rights reserved.
doi:10.1016/j.cej.2008.01.018

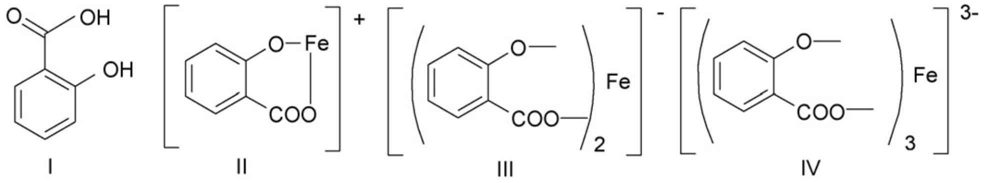

Fig. 1. Structural formulas of SA (I) and complexes of SA with Fe^{3+} (II–IV).

(classical Fenton system). Recently several modifications of classical Fenton were successfully applied for water and soil decontamination.

Modified Fenton reactions have been used to solve apparent disadvantages in the use of classical Fenton, including costly acidic range needed to maintain the radical reactions, handling problems associated with hygroscopic character and readily oxidised iron (II) salts and formation of secondary pollution [14]. There are several ways to modify classical Fenton system. Some modifications are mentioned hereafter.

For example, some researches use ferric ion as the catalyst when high hydrogen peroxide concentrations are applied [15,16]. With high hydrogen peroxide concentrations, iron (II) is rapidly oxidised to iron (III), resulting in immediate consumption of hydrogen peroxide residual. Iron (III) application can reduce hydrogen peroxide consumption creating aggressive conditions for effective contaminants oxidation. The application of iron oxide minerals (hematite α-Fe_2O_3, goethite α-FeOOH, magnetite Fe_3O_4 and ferrihydrite) as the catalysts in hydrogen peroxide oxidation of organic compounds is also effective because of consistent rates of hydroxyl radical generation at high concentrations of hydrogen peroxide used [17–20]. In addition, α-FeOOH/H_2O_2 system has the advantages over the homogeneous Fe^{2+}/H_2O_2, Fe^{3+}/H_2O_2 systems from the viewpoint of reaction pH range and the removal of iron. The application of novel, highly stable and active heterogeneous catalysts (Fe_2O_3 or Fe supported into SBA-15 mesostructured material, etc.) and increasing of the process temperature up to 80–120 °C, so-called catalytic wet hydrogen peroxide oxidation process, can be also a very effective modification of the classical Fenton system for degradation of a wide range of organic compounds in water [21,22]. The application of iron chelates (typically organic acids) can promote chemical oxidation of contaminants by formation of iron–chelate complexes [15,23]. The primary advantage of these complexes is the potential for the effective generation of hydroxyl radicals at near-neutral pH [23]. In addition, most of the chelating agents are natural products that are readily degraded by microorganisms. Thus, this Fenton modification is not pose an environmental concern and can be directly compatible with biodegradation process [15]. Hydrogen peroxide can be also decomposed by most ions of transition metals (Cu, Zn, Mn, etc.) and by minerals of those metals [24]. These other metals have not been found as efficient as iron in terms of their potential to create oxidising conditions. Nevertheless, they are very important since natural and atmospheric water may contain large quantities of these species.

The application of Fenton oxidation technology for SA-contaminated water purification can face one major obstacle: formation of intensely coloured stable complexes between SA and Fe^{3+} [25] that may influence SA degradation by Fenton oxidation. The violet complex, tetraaquosalicylatroiron (III) complex, (Fig. 1, II) is formed under pH 1 and is characterized by peak absorption at the wavelength of 530 nm. The reddish-violet complex (Fig. 1, III) is formed under pH 2.5 and has the maximum absorption at 480 nm. Finally, the yellow colour of the solution under pH 7.4 and the peak absorbance at the wavelength of 440 nm are indicative of another SA–Fe^{3+} complex formation (Fig. 1, IV).

There are some studies that have shown the negative effect of complex formation on organics oxidation or mineralization by Fenton/modified Fenton treatment [26,27]. For example, the application of cupric ions to H_2O_2/UV (maximum energy output at 254 nm) system was reported to considerably decrease the mineralization of humic acids due to the formation of humic acids–cupric complexes [26]. It was found that the humic acids–cupric complexes were more difficult to oxidize than the non-complexed form of humic acids. The most effective pH for SA mineralization was found to be 4.0 and the lowest effect was obtained at pH 6.0, while the removal efficiency at pH 9.0 was in between. This effect of pH on SA mineralization was associated with re-distribution between complexed and non-complexed forms of humic acids. In the study on azo dye degradation using the modified Fenton process [27] only partial decolourization by Fe^{2+}/UV and Fe^{2+}/H_2O_2 was achieved. It was mentioned by Kusic et al. [27] that this result might be attributed by the possible complex formation between Fe ions and dye by-products. However, the application of UV-irradiation (maximum energy output at 254 nm) to Fe^{2+}/H_2O_2 allowed achieving complete colour removal making a suggestion that Fe^{3+}/H_2O_2/UV system is able to destroy formed Fe ions-dye by-products complexes [27].

Only a few publications consider the application of modified photo-assisted Fenton system for SA degradation. For instance, the photodegradation of SA in aqueous dispersions of α-FeOOH/H_2O_2 at neutral pH was investigated [28,29]. It was found that the SA photodegradation process occurs not via a photosensitization process, involving an electron injection from an excited organic to α-FeOOH particle, but directly via the photoexcitation of the complex H_2O_2 with α-FeOOH particles. Moreover SA underwent rapid decomposition and mineralization in α-FeOOH/H_2O_2/UV system due to its strong ability to complex with surface iron atoms of goethite. The photo-assisted Fenton degradation of SA by using Fe ions on strongly acidic ion exchange resin (SAIER) as catalyst was studied [30]. The results indicated that the Fe/SAIER catalyst considerably enhance the degradation rate of SA without remarkable Fe leaching to the solution, suggesting that the catalyst has photocatalytic activity. There are no any studies on the applicability of mineral-catalysed modified Fenton system without UV-irradiation for SA degradation. Only one study [31] on the application of classical Fenton for the SA degradation was performed. The main target of that study was to examine the method for indirect determination of the concentration of hydroxyl radicals in aqueous solution by the quantitation of primary hydroxylated derivates of SA (2,3-dihydroxybenzoic acid, 2,5-dihydroxybenzoic acid and catechol) formed during the oxidation by Fenton's reagent. The influence of hydrogen peroxide and catalyst concentrations as well as the effect of possible SA–iron complex formation on SA degradation was not assessed in that research.

The main objective of the present study was to test the ability of classical Fenton system (Fe^{2+}/H_2O_2) and its modifications using $Fe_2(SO_4)_3$ or α-FeOOH as source of iron catalyst to degrade SA in water. The effect of UV irradiation addition (with maximum energy output at a wavelength of 254 nm) to Fe^{2+}/H_2O_2, Fe^{3+}/H_2O_2 and α-FeOOH/H_2O_2 systems, both at low or high dosages of catalyst applied for SA degradation was evaluated. The influence of SA/H_2O_2 and SA/Fe^{2+} ratios in classical Fenton system and aqueous solution pH in α-FeOOH/H_2O_2 on SA degradation was assessed. Among the factors that may affect SA degradation by Fenton/modified Fenton SA–iron complexation was considered. The effect of the applied treatment methods on overall COD and BOD reduction and biodegradability (BOD/COD) was evaluated.

2. Experimental

SA, purchased from Aldrich Co., was of analytical grade. The solutions were prepared dissolving SA in twice-distilled water. The initial concentration of SA in all experiments was 4 mM. All experiments were carried out at $20 \pm 1\,^{\circ}C$ and repeated.

Fenton (Fe^{2+}/H_2O_2), photo-Fenton (Fe^{2+}/H_2O_2/UV) and modified Fenton treatment (Fe^{3+}/H_2O_2, Fe^{3+}/H_2O_2/UV, α-FeOOH/H_2O_2 and α-FeOOH/H_2O_2/UV) were performed in the batch mode. In Fenton, photo-Fenton and modified Fenton treatment the pH was adjusted to 3.0, if not specified otherwise. The adjusting of pH was done with 0.1 and 1.0N solution of H_2SO_4 or 0.1 and 1.0N NaOH. A standard procedure consisted of treating 1.2 L of fresh SA solution in the cylindrical glass reactor with magnetic stirring.

A mercury low-pressure OSRAM lamp with an energy input of 10 W located inside the reactor in quartz tube was used as an UV-source during photo-Fenton/modified photo-Fenton treatment. The UV-irradiation intensity at 254 nm measured with potassium ferrioxalate actinometry [32] was 3.20 ± 0.07 μEinstein/s. The lamp was turned on at least 10 min advance to insure constant output. The reactor was maintained at desired temperature $20 \pm 1\,^{\circ}C$ using cooling jacket and the temperature was controlled by the thermometer immersed to the solution.

Different concentrations of Fe^{2+} (from 0.25 to 1.6 mM), Fe^{3+} (from 0.25 to 0.5 mM) or α-FeOOH (from 0.15 to 1.0 g/L) and H_2O_2 (from 4 to 16 mM) were used in these experiments. Ferrous sulphate ($FeSO_4 \cdot 7H_2O$), ferric sulphate ($Fe_2(SO_4)_3 \cdot 9H_2O$) and goethite (98% <5 μm) were used as sources of iron in applied Fenton/modified Fenton treatments. Goethite (catalyst grade), purchased from Aldrich Co., was used without any pretreatment. SA solution and α-FeOOH were magnetically stirred for ca. 30 min prior to H_2O_2 addition to ensure the establishment of sorption/desorption equilibrium of organics on the surface of goethite. At time intervals the samples were withdrawn from the reactor and filtered through a Millipore filter (0.45 μm). The reaction was stopped by adding 10% aqueous solution of Na_2SO_3. Oxidation experiments were conducted using duplicates. Results are presented including ± standard deviation of the mean ($n = 2$).

The degradation of SA was followed with a HPLC microchromatograph CLAS MPm coupled with UV–vis detector SAPHIRE. Ten microliters were injected to microcolumn MAG 0 (1.5 mm × 150 mm), filled with Biospher PSI 100 C18, 5 μm. The isocratic method with a solvent mixture of 40% acetonitrile and 0.2% of acetic acid in water and the flow rate of 70 μL/min was applied. The retention time for SA was 5.5 min and the detection wavelength of 296 nm.

After the designated Fenton/modified Fenton oxidation time, milk of lime (10%) was added (1.4 g CaO/L of treated solution) to raise the pH to a level where dissolved ferrous iron is precipitated as ferric hydroxide. Then the solution was left for the sedimentation up to 24 h and further filtered through a paper (blue ribbon) filter. After this post-treatment COD and BOD values of the supernatant were measured indicating their reduction in overall treatment processes.

Total dissolved iron concentration in bulk solution during the modified Fenton treatment used goethite as source of iron catalyst and in the post-treated solutions was measured photometrically with 1,10-phenanthrolinium chloride (Heλios UV–vis spectrophotometer, Thermo Electron Corporation, UK) at 492 nm [33]. The residual concentration of hydrogen peroxide after Fenton/modified Fenton treatment and the post-treatment described above was measured photometrically (Heλios UV–vis spectrophotometer) at 410 nm as a complex with Ti^{4+} [34]. Hydrogen peroxide was not found in the samples sent to COD and BOD analyses.

COD was determined by closed reflux, titrimetric method [35]. In addition, the 7-day biochemical oxygen demand of the initial and treated solutions of SA was determined [35]. Dissolved oxygen was measured before and after incubation using the membrane electrode method with Marvet Junior oxygen analyser (model MJ2000).

3. Results and discussion

3.1. Degradation of salicylic acid by Fenton treatment and its modifications

Fenton and modified Fenton were applied for the degradation of SA. In Fenton treatment, both the concentration of hydrogen peroxide and the catalyst (Fe^{2+}) affected the degradation of SA. Relatively high molar ratios of H_2O_2 to SA in Fenton treatment were favourable when keeping hydrogen peroxide/catalyst molar ratio constant at 10:1 (Fig. 2, where C and C_0 are SA

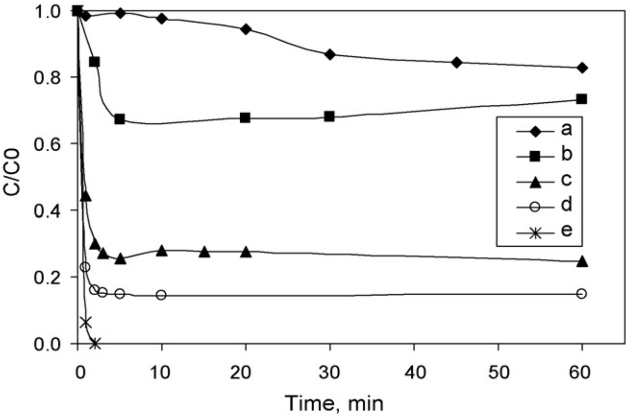

Fig. 2. Degradation of SA by Fenton treatment (pH 3.0) at the molar ratio of H_2O_2/Fe^{2+} = 10:1 and different molar ratios of SA/H_2O_2, where (a) 1:1, (b) 1:2, (c) 1:2.5, (d) 1:3, and (e) 1:4.

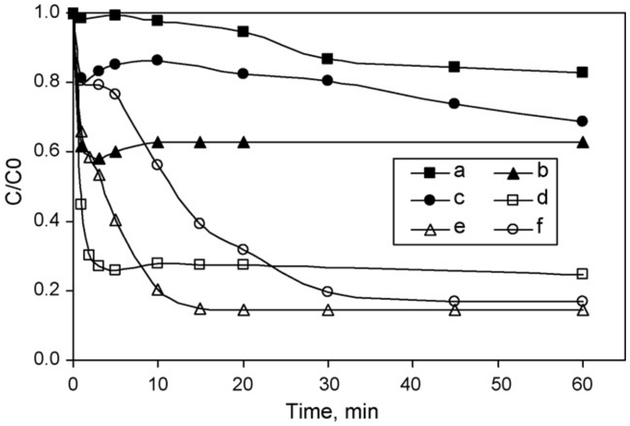

Fig. 3. Degradation of SA by Fenton treatment (pH 3.0) at different molar ratios of $SA/H_2O_2/Fe^{2+}$, where (a) 1:1:0.1, (b) 1:1:0.05, (c) 1:1:0.025, (d) 1:2.5:0.25, (e) 1:2.5:0.125, and (f) 1:2.5:0.0625.

concentrations at given treatment time and zero reaction time, respectively), as the degradation time of SA was considerably shortened with the increase of H_2O_2 concentration. For example, when H_2O_2 admixture was 16 mM (SA/H_2O_2 = 1:4), complete degradation of SA (100%) was achieved in 1–2 min only. Lower ratios of H_2O_2 to SA (from 2:1 to 3:1) did not allow achieving complete degradation of SA in Fenton treatment. The degradation was fast at the initial stage of the treatment but then stopped.

The residual concentration of hydrogen peroxide measured immediately after the treatment was 6–8% of the initial value, which could not be the reason of reaction termination. It can be supposed that SA degradation by Fenton treatment was retarded by formation of stable complex between Fe^{3+} (formed by the oxidation of ferrous iron during the Fenton reaction) and the residual target compound. Similar negative effect of humic acids–cupric complexes on humic acids mineralization by application of Cu^{2+}/H_2O_2/UV was observed by Liao et al. [26].

The formation of the complexes was observed by the change in reaction mixture colour to dark violet and monitored spectrophotometrically (the wavelength scan over a range of 400–600 nm). The violet colour and the maximum peak absorbance at a wavelength of 530 nm are indicative of complex II (Fig. 1) formation. However, other complexes of SA–Fe^{3+} (Fig. 1) were also formed. Moreover, ferric iron generated during the oxidation of ferrous iron could be bonded by the formation of different complexes with salicylic acid degradation by-products. Besides the primary derivates of SA, such as 2,3-dihydroxybenzoic acid, 2,5-dihydroxybenzoic acid and catechol [12,31] the major by-products of SA degradation are various organic acids, such as muconic, oxalic and malonic [8,10,12,13] that have a tendency to complexation.

In the case of Fenton treatment with the molar ratio of H_2O_2/SA = 1:1, SA degradation was retarded and further terminated also due to the low concentration of hydrogen peroxide. The residual concentration of H_2O_2 measured immediately after the treatment (60 min) was zero in this case.

Due to the tendency of SA to form complexes, decreasing the concentration of Fe^{2+} intensified SA degradation. As can be seen in Fig. 3 (cases b and e), a two-fold decrease of Fe^{2+} (H_2O_2/Fe^{2+} = 20:1) at constant SA/H_2O_2 ratio considerably reduce SA concentration but did not allow achieving complete degradation. The study of Liao et al. [26] also indicated that the reduction of cupric ion concentration showed the positive effective in humic acids mineralization by Cu^{2+}/H_2O_2/UV.

A further two-fold reduction of the catalyst concentration (H_2O_2/Fe^{2+} = 40:1) did not accelerate the degradation of SA; however, it allowed achieving approximately the same SA degradation degree as in the previous case within longer treatment time (Fig. 3, cases c and f). The possible reason is that low concentrations of Fe^{2+} retard SA–Fe^{3+} complexation due to insufficient ferric iron formation allowing hydroxyl radicals to attack the non-complexed SA. This was clearly observed at high H_2O_2/SA molar ratios (2.5:1).

Usually, enhancement of organic decomposition is observed during the photo-Fenton. This is probably due to photolysis of aqueous complex $Fe(OH)^{2+}$, which is an important source of $OH^{\bullet}$ (Eq. (1)).

$$Fe(OH)^{2+} + UV \rightarrow OH^{\bullet} + Fe^{2+} \qquad (1)$$

In addition, the photolysis of $Fe(OH)^{2+}$ regenerates the oxidised Fe^{2+}, so the photo-enhanced Fenton process needs lower Fe^{2+} dosages compared with the conventional Fenton process [36]. However, the present study demonstrated that UV-irradiation with the maximum energy output at a wavelength of 254 nm did not substantially improve the action of the Fenton's reagent system (Fig. 4). Several reasons may be responsible for retardation in the degradation of SA by photo-Fenton treatment making the degradation close to that (Fig. 4, cases c and d) or even slower (Fig. 4, cases e and f) than in the Fenton treatment. Firstly, SA–iron complexes have a strong absorption at 254 nm; weaken the intensity of photonic flux on aqueous complex $Fe(OH)^{2+}$ by acting as an inner filter. The photoexciting of the complex (Eq. (1)), which is the initial step in the homogeneous photo-Fenton mechanism, is therefore hindered. Secondly, the competitive complex formation between SA with Fe^{3+} (Fig. 1) and $OH^{\bullet}$

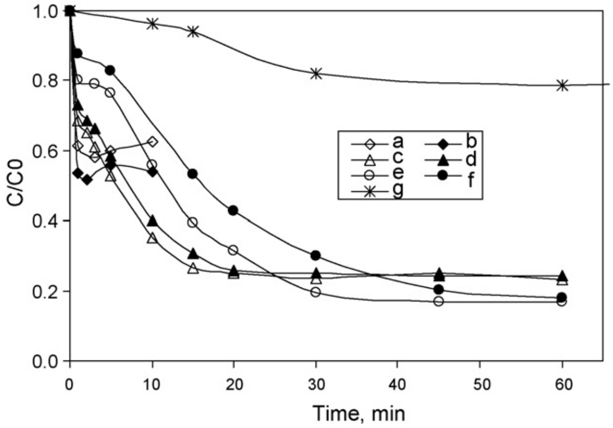

Fig. 4. Degradation of SA by Fenton/photo-Fenton treatment (pH 3.0) at different molar ratios of $SA/H_2O_2/Fe^{2+}$, where (a) 1:1:0.05, (b) 1:1:0.05 + UV, (c) 1:2:0.1, (d) 1:2:0.1 + UV, (e) 1:2.5:0.0625, (f) 1:2.5:0.0625 + UV, and (g) UV only.

with Fe^{2+} (Eq. (2)) also may influence the degradation of SA.

$$Fe^{2+} + OH^{\bullet} \rightarrow Fe(OH)^{2+} \quad (2)$$

Slight acceleration of SA degradation in the first stage of photo-Fenton oxidation with subsequent termination was observed at higher molar ratios of $H_2O_2/SA = 2.5:1$ and $H_2O_2/Fe^{2+} = 40:1$ (Fig. 4, cases a and b) only. However, the same final SA degradation degree was achieved in both Fenton and photo-Fenton reactions (Fig. 4). Application of photo-Fenton was found unreasonable as more complicated and, therefore, costly method. Low reduction in SA concentration (10 ± 1% for 60 min) was observed when the UV-irradiation alone was applied (Fig. 4, case g).

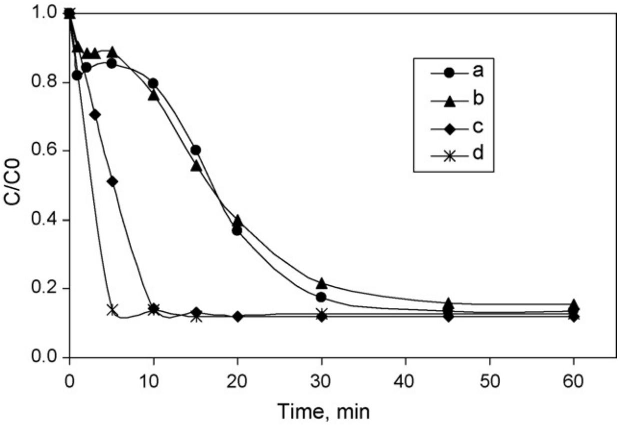

Fig. 5. Degradation of SA by modified Fenton/photo-Fenton treatment (pH 3.0) at different molar ratios of $SA/H_2O_2/Fe^{3+}$, where (a) 1:2.5:0.0625, (b) 1:2.5:0.0625 + UV, (c) 1:2.5:0.125, and (d) 1:2.5:0.125 + UV.

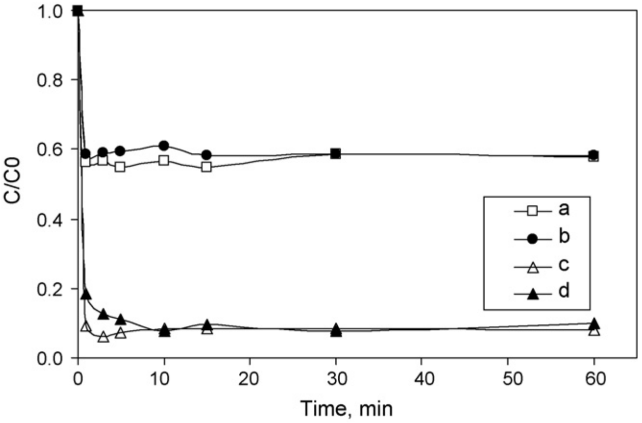

Fig. 6. Degradation of SA by modified Fenton (α-FeOOH/H_2O_2) and modified photo-Fenton (α-FeOOH/H_2O_2/UV) treatment (pH 3.0), where (a) $SA/H_2O_2 = 1:4$, α-FeOOH 0.15 g/L; (b) $SA/H_2O_2 = 1:4$ + UV, α-FeOOH 0.15 g/L, (c) $SA/H_2O_2 = 1:4$, α-FeOOH 1.0 g/L, and (d) $SA/H_2O_2 = 1:4$ + UV, α-FeOOH 1.0 g/L.

Modified Fenton/photo-Fenton (with $Fe_2(SO_4)_3$ or α-FeOOH as source of iron) was also applied for SA degradation (Figs. 5 and 6). If only ferric iron is originally present, it can be regenerated via reactions (3)–(5) to ferrous iron required for catalyzing of H_2O_2 decomposition with the following hydroxyl radical formation [20]:

$$Fe^{3+} + H_2O_2 \rightarrow Fe^{2+} + HO_2^{\bullet} + H^+ \quad (3)$$

$$HO_2^{\bullet} \leftrightarrow O_2^{\bullet -} + H^+ \quad (4)$$

$$HO_2^{\bullet} + Fe^{3+} \rightarrow Fe^{2+} + O_2 + H^+ \quad (5)$$

A two-fold increase in ferric iron initial concentration (from 0.25 to 0.5 mM) allowed accelerating SA degradation resulting in the same degradation degree of SA (82%) in shorter time (Fig. 5). The degradation of SA was not improved by addition of UV-irradiation to Fe^{3+}/H_2O_2 system. This effect was similar to that observed in the Fenton coupled with UV-irradiation. Moreover, the application of Fe^{3+}/H_2O_2 and Fe^{3+}/H_2O_2/UV led to the same degradation degree of SA as in classical Fenton treatment with following termination, where the entire residual SA is complexed with Fe^{3+}. The substantial SA degradation (85–88%) in the first stage (prior to the termination) of the treatment suggests that reactions (3)–(5) are considerably faster than complex formation.

In mineral-catalysed Fenton oxidation SA degradation took place mostly in the first stage (1–3 min) of the treatment (Fig. 6). Further SA–Fe^{3+} complex formation on solid and solute phases terminated SA degradation because iron complexes cannot catalyse H_2O_2 to produce reactive species. The termination in SA degradation after 1–3 min of the treatment was observed under all pH conditions and goethite dosages applied.

In general a reaction mechanism in mineral-catalysed Fenton incorporates a single rate limiting step controlling H_2O_2 loss and ultimately contaminant degradation, superoxide and hydroxyl radical formation, scavenging reactions of oxygen radicals with the metal-oxide surface and contaminant degradation by reaction with hydroxyl radicals that are formed by both surface and solution reactions [37]. In surface reactions mechanism the overall reaction rate will include various steps such as diffusion of chemicals to the surface, surface complex formation (that is, specific adsorption on the reactive sites), actual electron transfer, dissociation of the successor complex (that is, desorp-

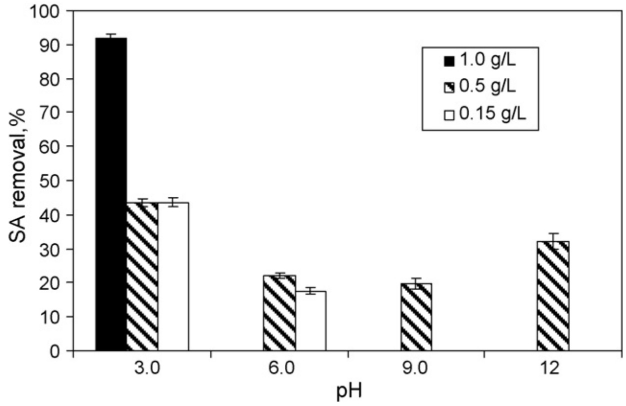

Fig. 7. SA removal (%) by modified Fenton treatment ($SA/H_2O_2 = 1{:}4$, M/M) at different initial pH values and goethite loads.

tion of products), and (re)generation of the reactive sites [38]. The first-order relationship with respect to the concentrations of H_2O_2 and α-FeOOH indicating the rate-determining step in hydrogen peroxide decomposition is presented in Eq. (6) [38].

$$\equiv Fe^{III}OH + H_2O_2 \rightarrow \equiv Fe^{II}{-}OH_2 + HO_2^{\bullet} \tag{6}$$

The effect of goethite load on the degradation of SA by α-FeOOH/H_2O_2 treatment at constant molar ratio of $SA/H_2O_2 = 1{:}4$ is shown in Fig. 7. The increase of goethite load from 0.15 to 0.5 g/L at pH 3.0 did not affect the degradation and resulted in 43 ± 1% SA removal. In contrast to Fenton treatment, considerable increase of catalyst concentration (goethite load increased from 0.5 to 1.0 g/L) improved the degradation and resulted in highest (92 ± 1%) removal of SA by α-FeOOH/H_2O_2 under acidic conditions. The residual concentration of hydrogen peroxide – 22.5% of the initial 16 mM – was also the lowest among all the treatments with different dosages of goethite used under acidic conditions. In the experiments without hydrogen peroxide addition and at pH 3.0, adsorption of SA on the surface of goethite was 10.8 ± 1.7% at high goethite load (1.0 g/L) and less than 1% at low goethite dosages (0.15 and 0.5 g/L).

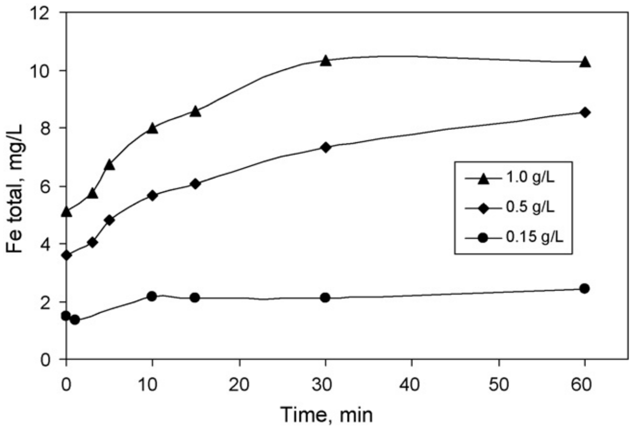

Fig. 8. Effect of goethite load on iron dissolution in modified Fenton treatment of SA ($SA/H_2O_2 = 1{:}4$ M/M, pH 3.0).

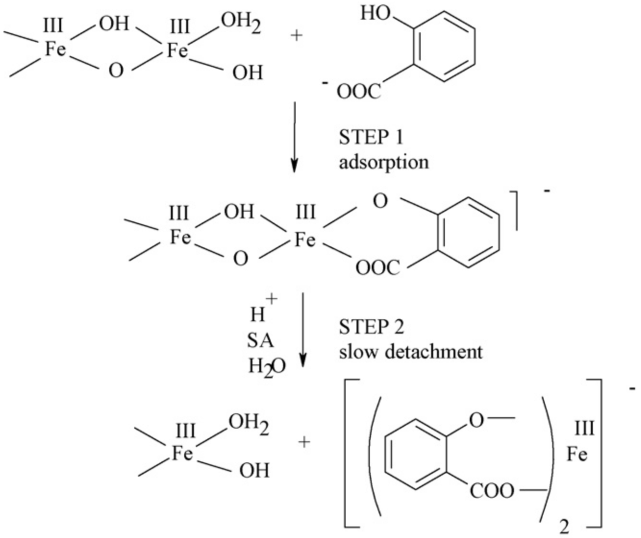

Fig. 9. Iron dissolution mechanism from goethite by complexation in the presence of SA.

The dissolution of iron under acidic conditions and at different dosages of goethite ($SA/H_2O_2 = 1{:}4$) is described in Fig. 8. At zero-reaction time sufficient concentration of dissolved iron for catalyzing hydrogen peroxide decomposition was found in bulk solution. The amount of dissolved iron considerably increased during the treatment especially at high dosages (0.5 and 1.0 g/L) of goethite. Thus large amounts of iron dissolution at the acidic conditions reduced the concentration of iron oxide and change the mechanism of the reaction from the surface based to the solution based.

In general the dissolution mechanisms of iron from iron minerals can be classified according to the solutant type and the reaction that takes place prior to dissolution. Three dissolution mechanisms are distinguished: protonation, complexation, and reduction [39]. In the case of SA the dissolution mechanism by complexation is obviously has to be prevalent. This was also shown by He et al. [28]. Dissolution by complexation involves attachment of a compound (other than H^+) onto the crystal surface. Sometimes protonation (Eq. (7)) is required prior to complexation, where a strongly complexing ligand in the solution is replaced by a protonated OH-group bound to the substrate.

$$\alpha\text{-FeOOH} + 3H^+ \rightarrow Fe^{3+} + 2H_2O \tag{7}$$

The surface ion–ligand complex ultimately detaches into the aqueous phase [39]. High polarity of iron (hydr)oxides surface complex will lead to a decrease in bond strength between the surface iron and its neighbouring atoms, which facilitates iron dissolution. A possible mechanism by which SA is complexing with surface iron atoms of goethite is shown in Fig. 9.

Experiments to study the influence of pH on the treatment of SA by α-FeOOH/H_2O_2 were carried out (Fig. 7). SA could present in the solution in different forms—non-dissociated at pH < 3.0, and dissociated at pH 6.0–12 (the pK_a for SA is 2.97 [1]). As can be seen in Fig. 7, the highest removal of SA was observed at pH 3.0 (Fig. 7). The considerable increase in SA degradation (prior complex formation) under acidic conditions was probably achieved mainly by the leaching of iron in bulk

Table 1
BOD, COD values ± standard deviation of the mean and BOD/COD ratio for initial and treated SA solution

Ratios applied	COD (mg O/L)	BOD (mg O/L)	BOD/COD
Initial $[\mathrm{SA}]_0$ = 4 mM	880 ± 6	540 ± 8	0.6
$\mathrm{SA/H_2O_2/Fe^{2+}}$ = 1/1/0.025	664 ± 0	435 ± 10	0.7
$\mathrm{SA/H_2O_2/Fe^{2+}}$ = 1/1/0.05	560 ± 3	380 ± 6	0.7
$\mathrm{SA/H_2O_2/Fe^{2+/}UV}$ = 1/1/0.05/UV	540 ± 3	380 ± 12	0.7
$\mathrm{SA/H_2O_2/Fe^{2+}}$ = 1/2/0.05	362 ± 0	–	–
$\mathrm{SA/H_2O_2/Fe^{2+}}$ = 1/2/0.1	311 ± 0	190 ± 7	0.6
$\mathrm{SA/H_2O_2/Fe^{2+}/UV}$ = 1/2/0.1/UV	311 ± 0	180 ± 8	0.6
$\mathrm{SA/H_2O_2/Fe^{2+}}$ = 1/2.5/0.125	200 ± 7	120 ± 3	0.6
$\mathrm{SA/H_2O_2/Fe^{2+}}$ = 1/2.5/0.25	140 ± 0	90 ± 1	0.6
$\mathrm{SA/H_2O_2/Fe^{2+/}UV}$ = 1/2.5/0.0625/UV	136 ± 0	125 ± 2	0.9
$\mathrm{SA/H_2O_2/Fe^{2+}}$ = 1/3/0.3	95 ± 2	40 ± 1	0.4
$\mathrm{SA/H_2O_2/Fe^{2+}}$ = 1/4/0.4	70 ± 2	40 ± 2	0.6
$\mathrm{SA/H_2O_2/Fe^{3+}}$ = 1/2.5/0.125	282 ± 0	160 ± 1	0.6
$\mathrm{SA/H_2O_2/Fe^{3+}/UV}$ = 1/2.5/0.125/UV	230 ± 8	132 ± 13	0.6
$\mathrm{SA/H_2O_2/Fe^{3+}}$ = 1/2.5/0.0625	136 ± 0	110 ± 2	0.8
$\mathrm{SA/H_2O_2/Fe^{3+}/UV}$ = 1/2.5/0.0625/UV	175 ± 0	130 ± 5	0.7
$\mathrm{SA/H_2O_2}$ = 1/4, UV, α-FeOOH 0.15 g/L	669 ± 0	457 ± 1	0.7
$\mathrm{SA/H_2O_2}$ = 1/4, α-FeOOH 0.15 g/L	629 ± 0	426 ± 12	0.7
$\mathrm{SA/H_2O_2}$ = 1/4, α-FeOOH 0.5 g/L	594 ± 0	475 ± 10	0.8
$\mathrm{SA/H_2O_2}$ = 1/4, α-FeOOH 1.0 g/L	88 ± 0	76 ± 1	0.9
$\mathrm{SA/H_2O_2}$ = 1/4, UV, α-FeOOH 1.0 g/L	98 ± 8	80 ± 5	0.8
UV only	850 ± 3	–	–

(–) Not measured.

solution (Eq. (7)), which catalyse the decomposition of hydrogen peroxide with the subsequent formation of $\mathrm{OH^{\bullet}}$ (Eq. (3)).

Similar to the systems described above, UV-irradiation addition to α-$\mathrm{FeOOH/H_2O_2}$ treatment, both at low (0.15 g/L) or high (1.0 g/L) dosages of goethite and acidic conditions, did not promote the decomposition of SA (Fig. 6). High concentration of dissolved iron in bulk solution during SA degradation by goethite-catalysed photo-Fenton treatment at pH 3.0 made the presumption that the solution based mechanism was predominated.

Similar removal (20 ± 1%) of SA was achieved by modified Fenton treatment at the initial pH 6.0 and 9.0. The residual hydrogen peroxide was 52 ± 1% of the initial value in both cases after 60 min of treatment. Some increase in SA degradation degree (32 ± 2%) was observed at the initial pH 12. The observed positive effect in SA removal at pH 12 can be attributed to 11.5 ± 0.5% SA adsorption on the surface of goethite particles while at pH 3.0, 6.0 and 9.0 the adsorbed amount was less than 1%. Moreover, the decomposition rate of hydrogen peroxide during SA treatment at pH 12 was the highest and the residual concentration after 60 min of the treatment comprised 22.5%. This is supported by Chou and Huang [40] who observed that the rate constant of hydrogen peroxide decomposition on supported-iron oxide increased with pH. Thus, the oxidation of SA at these pH values probably occurred with $\mathrm{OH^{\bullet}}$ formed during decomposition of $\mathrm{H_2O_2}$ on the surface sites of α-FeOOH, as proposed by Lin and Gurol [38] because dissolved iron was not found in bulk solution. Thus, it can be concluded that the influence of pH on the reaction activity of goethite and the effect of surface and/or liquid complexes formation was also important.

The residual dissolved iron after Fenton/modified Fenton treatment was removed by milk of lime with consequent filtration; 0.1–5% of the initial value content remained.

3.2. *Effect of Fenton and its modification on overall COD and BOD reduction and biodegradability*

The initial biodegradability of SA in water was acceptable (BOD/COD = 0.6); however, further biodegradability improvement (up to BOD/COD = 0.9) was observed after Fenton/modified Fenton treatment with the following post-treatment (Table 1). Moreover, the application of these treatment methods allows achieving up to 90% of overall COD and BOD reduction in comparatively short treatment time. The overall reduction of COD and BOD was increased with increasing hydrogen peroxide and catalyst concentrations in classical Fenton treatment. Photo-Fenton treatment resulted in the similar overall reduction of COD and BOD values as Fenton with the same ratio of $\mathrm{H_2O_2/Fe^{2+}}$ and the subsequent post-treatment applied. Furthermore, the removal of SA in both treatment processes was also very similar (Fig. 4). This is probably due to the minor role of UV-irradiation in SA and its by-products degradation by photo-Fenton. The reduction of COD by UV-irradiation alone was negligible, suggesting that the synergism of catalyst and hydrogen peroxide is mostly responsible for COD reduction. Even though SA degradation degree in $\mathrm{Fe^{3+}/H_2O_2}$ treatment using 0.25 and 0.5 mM of ferric iron were similar (Fig. 5), overall COD reduction was somewhat lower when high (0.5 mM) catalyst concentration was applied, resulting in less biodegradable by-products formation. A similar effect on overall COD reduction and biodegradability was observed after the application of modified photo-Fenton treatment when the concentration of Fe^{3+} was doubled from 0.25 to 0.5 mM ($SA/H_2O_2/Fe^{3+} = 1:2.5:0.0625$ and $SA/H_2O_2/Fe^{3+} = 1:2.5:0.125$, respectively).

Overall COD and BOD reduction after modified Fenton/photo-Fenton treatment with α-FeOOH as iron catalyst source and the subsequent post-treatment with milk of lime was mostly lower than after Fe^{2+}/H_2O_2 or Fe^{3+}/H_2O_2 treatment application. Considerable reduction of overall COD and BOD values was achieved only at high dosages of goethite (1.0 g/L) applied under acidic conditions. The increase in biodegradability after the application of $\alpha\text{-FeOOH}/H_2O_2$ under acidic conditions and all goethite dosages used was obvious. However, the further optimization of this system from the viewpoint of effective SA removal in neutral pH range and usage of naturally occurring iron minerals in the absence of soluble iron is required.

4. Conclusions

The present study demonstrated that Fenton/modified Fenton were able to degrade SA in aqueous medium. SA–iron complex formation considerably affected SA degradation by all the treatment methods applied.

In the Fenton process, both the concentration of hydrogen peroxide and the catalyst (Fe^{2+}) influenced the degradation of SA. The degradation time of SA was considerably shortened with the increase of H_2O_2 concentration. A 100% reduction of SA was achieved in 1–2 min only when the molar ratio of $SA/H_2O_2/Fe^{2+}$ was 1:4:0.4. Due to the tendency of SA to form complexes with Fe^{3+}, lower ratios of $SA/H_2O_2/Fe^{2+}$ did not lead to complete degradation, resulting in up to 80% of SA removal. However, a two-fold reduction of the catalyst was favorable in this case.

Similar to the Fenton treatment the degradation of SA by modified Fenton was terminated by SA–iron complex formation. Fe^{3+}/H_2O_2 enabled to achieve the same SA degradation degree of SA as classical Fenton. Moreover, the application of Fe^{3+}/H_2O_2 treatment did not show any advantages in overall COD and BOD reduction compared with classical Fenton's reagent treatment.

The acidic pH conditions and high goethite load in modified Fenton used goethite as a catalyst source enabled SA decomposition of up to $92 \pm 1\%$. The considerable leaching of iron to bulk solution at pH 3.0 showed that the solution based mechanism in SA oxidation by $\alpha\text{-FeOOH}/H_2O_2$ was predominant. Some degradation of SA was observed at near-neutral (6.0) and higher pH values. Dissolved iron was not found in bulk solution at pH 6.0, 9.0 and 12 making a presumption that the surfaced based mechanism took place.

The photo-Fenton process did not accelerate the degradation of SA compared with the Fenton process. UV-irradiation addition to Fe^{3+}/H_2O_2 and $\alpha\text{-FeOOH}/H_2O_2$ systems, both at low or high dosages of catalyst applied, did not promote the decomposition of SA as well.

The post-treatment of the solution by milk of lime and subsequent filtration can easily reduce the residual iron in the aqueous phase to the level of less than 6.5 mg/L that is complied with the set requirements for wastewater discharge to local sewerage.

Even though the effect of iron catalyst type on biodegradability was not obvious, the application of all studied methods at the optimal conditions with the subsequent post-treatment by milk of lime addition allowed achieving up to 90% of overall COD and BOD reduction and considerable biodegradability improvement.

Acknowledgements

The financial support of the Estonian Science Foundation (grant 6564) is gratefully acknowledged. We thank Mr. Viktor Ahelik for his kind support in chromatographic analysis and technical assistance.

References

[1] INCHEM IPCS, Salicylic Acid. [http://www.inchem.org/documents/pims/pharm/pim642.htm], 31.08.2007.
[2] M. Windholz, S. Budavari, R.F. Blumetti, E.S. Otterbein (Eds.), The Merck Index, An Encyclopedia of Chemicals, Drugs and Biologicals, 10th ed., Merck & Co., Inc., Rahway, USA, New Jersey, 1983.
[3] R.L.M. Allen, Colour Chemistry, Appleton Century-Crafts, New York, 1971.
[4] W.H. Glaze, Drinking water treatment with ozone, Environ. Sci. Technol. 21 (1987) 224–230.
[5] K.T. Ranjit, I. Wilner, S.H. Bossmann, A.M. Braun, Lanthanide oxide doped titanium dioxide photocatalysts: effective photocatalysts for the enhanced degradation of salicylic acid and t-cinnamic acid, J. Catal. 204 (2001) 305–313.
[6] V. Vamathevan, R. Amal, D. Beydoun, G. Low, S. McEvoy, Photocatalytic oxidation of organics in water using pure and silver-modified titanium dioxide particles, J. Photochem. Photobiol. A 148 (2002) 233–245.
[7] K. Chhor, J.F. Bocquet, C. Colbeau-Justin, Comparative studies of phenol and salicylic acid photocatalytic degradation: influence of absorbed oxygen, Mater. Chem. Phys. 86 (2004) 123–131.
[8] C. Adán, J.M. Coronado, R. Bellod, J. Soria, H. Yamaoka, Photochemical and photocatalytic degradation of salicylic acid with hydrogen peroxide over TiO_2/SiO_2 fibres, Appl. Catal. A: Gen. 303 (2006) 199–206.
[9] O. Zahraa, S. Maire, F. Evenou, C. Hachem, M.N. Pons, A. Alinsafi, M. Bouchy, Treatment of wastewater dyeing agent by photocatalytic process in solar reactor, Int. J. Photoenergy (2006) 1–9.
[10] N. Karpel Vel Leitner, B. Delouane, B. Legube, F. Luck, Effects of catalysts during ozonation of salicylic acid, peptides and humic substances in aqueous solution, Ozone: Sci. Eng. 21 (1999) 261–276.
[11] M. Ernst, F. Lurot, J.-C. Schrotter, Catalytic ozonation of refractory organic model compounds in aqueous solution by aluminium oxide, Appl. Catal. B: Environ. 47 (2004) 15–25.
[12] C.K. Scheck, F.H. Frimmel, Degradation of phenol and salicylic acid by ultraviolet radiation/hydrogen peroxide/oxygen, Water Res. 29 (1995) 2346–2352.
[13] M. Yang, A. Xu, H. Du, C. Sun, C. Li, Removal of salicylic acid on peroskite-type oxide $LaFeO_3$ catalyst in catalytic wet air oxidation process, J. Hazard. Mater. 139 (2007) 86–92.
[14] D.F. Laine, I.F. Cheng, The destruction of organic pollutants under mild reaction conditions: a review, Microchem. J. 85 (2007) 183–193.
[15] R.J. Watts, S.E. Dilly, Evaluation of iron catalysts for the Fenton-like remediation of diesel-contaminated soils, J. Hazard. Mater. 51 (1996) 209–224.
[16] R.J. Watts, P.C. Stanton, Mineralization of sorbed and naph-phase hexadecane by catalyzed hydrogen peroxide, Water Res. 33 (1999) 1405–1414.
[17] R.J. Watts, M.D. Udell, S.W. Leung, Treatment of contaminated soils using catalysed hydrogen peroxide, in: W.W. Eckenfeld, A.R. Bowers, J.A. Roth

(Eds.), Chemical Oxidation Technologies for the Nineties, A Technomic Publishing Company, USA, Lancaster, 1992, pp. 37–50.

[18] A.L. Teel, C.R. Warberg, D.A. Atkinson, R.J. Watts, Comparison of mineral and soluble iron Fenton's catalysts for the treatment of trichloroethylene, Water Res. 35 (2001) 977–984.

[19] R. Andreozzi, V. Caprio, R. Marotta, Oxidation of 3,4-dihydroxybenzoic acid by means of hydrogen peroxide in aqueous goethite slurry, Water Res. 36 (2002) 2761–2768.

[20] W.P. Kwan, B.M. Voelker, Rates of hydroxyl radical generation and organic compound oxidation in mineral-catalyzed Fenton-like systems, Environ. Sci. Technol. 37 (2003) 1150–1158.

[21] J.A. Melero, G. Calleja, F. Martínez, R. Molina, M.I. Pariente, Nanocomposite Fe_2O_3/SBA-15: an efficient and stable catalyst for the catalytic wet peroxidation of phenolic aqueous solutions, Chem. Eng. J. 131 (2007) 245–256.

[22] G. Galleja, J.A. Melero, F. Martínez, R. Molina, Activity and resistance of iron-containing amorphous, zeolitic and mesostructured materials for wet peroxide oxidation of phenol, Water Res. 39 (2005) 1741–1750.

[23] J. Sun, J.J. Pignatello, Chemical treatment of pesticide wastes. Evaluation of Fe(III) chelates for catalytic hydrogen peroxide oxidation of 2,4-D at circumneutral pH, J. Agr. Food Chem. 40 (1992) 322–327.

[24] W.C. Schumb, C.N. Satterfield, R.L. Wentworth, Hydrogen Peroxide, Reinhold, New York, 1955.

[25] I.M. Korenman, Photometric Analyse. Determination Methods of Organic Compounds, Khimija, Moscow, Russia, 1975, pp. 265–266 (in Russian).

[26] C.H. Liao, M.C. Lu, S.H. Su, Role of cupric ions in the H_2O_2/UV oxidation of humic acids, Chemosphere 44 (2001) 913–919.

[27] H. Kusic, N. Koprivanac, L. Srsan, Azo dye degradation using Fenton type processes assisted by UV irradiation: a kinetic study, J. Photochem. Phtobiol. A 181 (2006) 195–202.

[28] J.u. Ju He, W. Ma, J. He, J. Zhao, J.C. Yu, Photooxidation of azo dye in aqueous dispersions of H_2O_2/α-FeOOH, Appl. Catal. B: Environ. 39 (2002) 211–220.

[29] J.u. Ju He, W. Ma, W. Song, J. Zhao, X. Qian, S. Zhang, J.C. Yu, Photoreaction of aromatic compounds at α-FeOOH/H_2O interface in the presence of H_2O_2: evidence for organic-goethite surface complex formation, Water Res. 39 (2005) 119–128.

[30] J. Feng, X. Hu, P.L. Yue, Degradation of salicylic acid by photo-assisted Fenton reaction using Fe ions on strongly acidic ion exchange resin as catalyst, Chem. Eng. J. 100 (2004) 159–165.

[31] J.-F. Jen, M.-F. Leu, T.C. Yang, Determination of hydroxyl radicals in an advanced oxidation process with salicylic acid trapping and liquid chromatography, J. Chromatogr. A 796 (1998) 283–288.

[32] A.J. Gordon, R.A. Ford, A Handbook of Practical Data, Techniques and References, The Chemist's Companion, Wiley-Interscience Publication, New York, 1972, pp. 373–376.

[33] E. Merck, The Testing of Water, ninth ed., Darmstadt, Germany, 1974, pp. 108–110.

[34] G.M. Eisenberg, Colorimetric determination of hydrogen peroxide, Ind. Eng. Chem. Res. 15 (1943) 327–328.

[35] L.S. Eaton, E.W. Clesceri, A.E. Rice, Greenberg (Eds.), Standard Methods for the Examination of Water & Wastewater, 21st ed., American Public Health Association, American Water Works Association, Water Environment Federation, USA, 2005, pp. 5-2–5-18.

[36] M. Yang, J. Hu, K. Ito, Characteristics of Fe^{2+}/H_2O_2/UV oxidation process, Environ. Technol. 19 (1998) 183–191.

[37] C.M. Miller, R.L. Valentine, Mechanistic studies of surface catalyzed H_2O_2 decomposition and contaminant degradation in the presence of sand, Water Res. 33 (1999) 2805–2816.

[38] S.S. Lin, M.D. Gurol, Catalytic decomposition of hydrogen peroxide on iron oxide: kinetics, mechanisms, and implications, Environ. Sci. Technol. 32 (1998) 1417–1423.

[39] G. Sposito, The Chemistry of Soils, Oxford University Press, New York, 1989, p. 27.

[40] S. Chou, C. Huang, Decomposition of hydrogen peroxide in a catalytic fluidized-bed reactor, App. Catal. A 185 (1999) 237–245.